JOURNAL OF MATERIALS SCIENCE 30 (1995) 1801–1806

A comparative evaluation method of machinability for mica-based glass-ceramics

D. S. BAIK, K. S. NO, J. S. CHUN
Department of Materials Science and Engineering, Korea Advanced Institute of Science and Technology, Taejon 305-701 Korea

Y. J. YOON
Division of Electrical Materials, Korea Electrotechnology Research Institute, Changwon 641-120, Korea

H. Y. CHO
Department of Precision Mechanical Engineering, Choongbuk National University, Cheongju 360-763, Korea

The machinability of mica glass-ceramics is evaluated using a tool dynamometer. Several samples with different chemical compositions and microstructures were tested in turning operations using TiCN cermet tools. The cutting rate dependence of specific cutting energy has been studied to find a simple method for the evaluation of machinability. The mechanical strength, the surface roughness of the machined surface and the fracture toughness were measured to support the machining behaviour. For the determination of machinability, the specific cutting energy at low cutting rate conditions, neglecting an elastic impact effect, and the slope of the log–log plot of the specific cutting energy versus cutting rate were considered as the reasonable parameters. These results are correlated with the microstructure and the hardness of the workpiece. In particular, the microhardness of the sample is shown to control the cutting characteristic.

1. Introduction

There is a family of nonporous machinable glass-ceramics based on fluorine-containing mica crystals [1–3]. These materials contain highly interlocked mica crystals in a glass matrix, which facilitates continuous cutting without macroscopic fracture. Since mica can be readily delaminated due to its low cleavage energy, fractures propagate parallel to the flat crystals. The random intersections of the crystals cause crack deflections, branching and blunting which help to prevent microscopic fractures from propagating beyond the local cutting area. These glass-ceramics can be machined to very high precision ($\pm$ 10 μm) using regular high-speed tools.

The machinability is broadly understood as the ease with which a material is cut. It is easily appreciated but not readily measured in quantitative terms. Various criteria, such as measuring tool wear, surface roughness and cutting force, may be employed in judging the machinability [4].

The machinability of mica glass-ceramics can vary over a wide degree according to their microstructures and compositions. The objectives of this paper are to introduce the concept of the cutting energy per unit volume in order to evaluate the machinability of the mica-based glass-ceramics and to propose a simple model which enables the comparison of the machinabilities among mica-based glass-ceramics.

2. Experimental procedure

Samples for the machinability test are fluorophlogopite-based glass-ceramics with different chemical compositions and thermal treatments. The composition of the base glass is SiO_2 50%, Al_2O_3 20%, MgO 15%, K_2O 8%, Li_2O 0.9%, F 6.1% by weight. Other dopants, such as TiO_2, ZrO_2 and B_2O_3, were added to modify the microstructure and the crystallinity. The raw materials were mixed in a ball mill with alumina balls, melted in Pt–10% Rh crucibles at 1550 °C for 2 h and cast on a steel mould preheated to 500 °C. The machinability test samples were cut to 25 × 25 × 90 mm^3 bars, heat-treated and then machined to 22 mm diameter rods. All samples were heat-treated at 680 °C for 2 h to provide enough nucleation, and the temperature was increased to the crystallization temperature at the rate of 2 °C min^{-1}. A commercial material, MACOR® (Corning Glass Works, USA), was used as a reference for good machinability. The physical specifications of test samples are listed in Table I.

Cutting forces were measured using 3-component type strain gauges attached to a tool dynamometer (TD-500KA Kyowa, Japan) during the turning operation without lubrication. The signals from the strain gauges were amplified, plotted and the cutting forces calculated. The 3-component forces, principal component (F_p), axial component (F_a), and radial component (F_r), are described in Fig. 1. The tool was

0022–2461

TABLE I The materials' data of mica glass-ceramics used in cutting tests

Sample	Composition[a]	Heat treatment (°C h^{-1}) + 680/2	Crystallinity (%) Microstructure[b]	Hardness (GPa)	MOR (MPa)	K_{Ic} (MPa/m$^{1/2}$)	γ_{eff} (J m^{-2})
1	U	900/6	60 NI	4.5 ± 0.3[c]	80.7 ± 8	1.06 ± 0.2	12.6
2	U	950/2	71.6 I	5.56 ± 0.6	–[d]	–	–
3	U	1100/2	77.4 I	5.11 ± 0.8	–	–	–
4	Z	900/6	49.5 NI	5.4 ± 1	54.3 ± 10	1.2 ± 1.2	16.2
5	Z	950/2	53 NI	6.7 ± 0.7	–	–	–
6	Z	1100/6	78 HI	3.3 ± 0.2	128.1 ± 7	1.29 ± 0.2	18.7
7	ZB	900/6	75 I	5.2 ± 0.3	56.3 ± 11	0.91 ± 0.2	9.3
8	ZB	950/2	70.8 NI	6.01 ± 0.4	–	–	–
9	ZB	1000/6	53.8 NI	4.91 ± 0.5	134.7 ± 31	0.93 ± 0.1	9.7
10	ZB	1050/6	61 I	5.61 ± 0.4	147 ± 34	1.12 ± 0.1	14.2
11	ZB	1100/6	73 I	3.08 ± 0.23	149.4 ± 19	1.6 ± 0.4	28.8
12	T3	1100/6	72.9 I	3.43 ± 0.2	72 ± 10	1.42 ± 0.3	22.7
13	T5	900/6	65 NI	6.86 ± 0.4	–	–	–
14	T5	950/2	> 80 I	5.72 ± 0.3	–	–	–
15	T5	1100/2	> 80 I	4.17 ± 0.2	–	–	–
16	MACOR®			2.0 ± 0.3			

[a]U, Undoped base composition; Z, 3 wt % ZrO_2 doped; ZB, 3 wt % ZrO_3 and 2 wt % B_2O_3 doped; T3, 3 wt % TiO_2 doped, T5, 5 wt % TiO_2 doped.
[b]NI, Not interlocked mica structure; I, Interlocked; HI, Highly interlocked.
[c]The errors represent standard deviations.
[d]– Not measured.

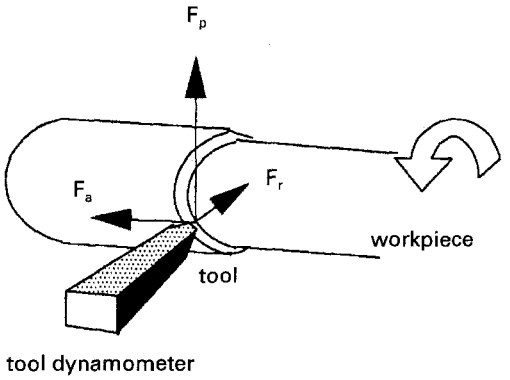

Figure 1 3-component forces of cutting.

TABLE II Cutting conditions and tool specifications

Operation	turning of rod sample
Depth of cut	0.5 mm
Feed rate	0.073 mm rev^{-1}
Sizes of specimen	20–30 mm (diameter) 130 mm (length)
Tool rake angle	15°
Revolving rate	60, 100, 165, 270, 350 580, 920 (r.p.m)
Tool	turning insert SNGG120408R from Korea Tungsten Co. rectangular clearance angle 0° nose radius 0.8 mm thickness 4 mm cutting edge length 12 mm Ti(C, N) cermet

a Ti(C, N)-based cermet having sharp eight-sided edges with a tip angle of 75°. At each measurement, a new edge was used to eliminate the error from the tip wear. The cutting condition and the tool specifications for the machinability test are listed in Table II.

Average maximum roughness, R_m was measured using a surface roughness tester (Seimitsu, Japan) in the axial direction to compare the degree of surface finishing. A microhardness tester with a diamond pyramid (Tukon 300BM, Page-Wilson Co. USA) was used to measure the microhardness. The load and loading time were 700 g and 15 s, respectively. Fracture toughness was measured by the indentation method [5]. Young's modulus was measured using the four-point bending test with an inner and outer span of 20 and 40 mm, respectively. Before the bending test, all specimens having sizes of 3 × 4 × 45 mm^3 were abraded with 30 grit SiC in a ball mill for 1 h. Moduli of rupture were determined by taking averages of 10 specimens at each point. Fracture surface energy was calculated by [6]

$$2\gamma_{eff} \approx \frac{K_{IC}^2}{E} \quad (1)$$

where γ_{eff} is effective surface energy, E is Young's modulus, and K_{IC} is the critical value of the stress intensity factor.

The microstructure and the crystallinity were observed using SEM (scanning electron microscope, Hitachi S2700, Japan) and XRD (X-ray diffractometer, Phillips, CuK_α, 40 kV, 30 mA). The X-ray background method [7] in the range 2θ = 10–17° provided the crystallinity of the glass-ceramics. The XRD patterns of the powder mixtures having the same compositions as the base glasses were used as references to compensate the background intensity. The error of crystallinity measurement in this experiment is less than ± 10% in the range between 20 and 65% and is larger than ± 10% in other ranges. Surface areas per unit weight of chip powders were measured by the BET (Brunauer–Emmett–Teller) method [8].

3. Results and discussion

In general, the cutting operation involves the removal of macroscopic chips in the form of ribbon and particles having a thickness of about 0.025–2.5 mm. The grinding operation usually involves the subdivision of

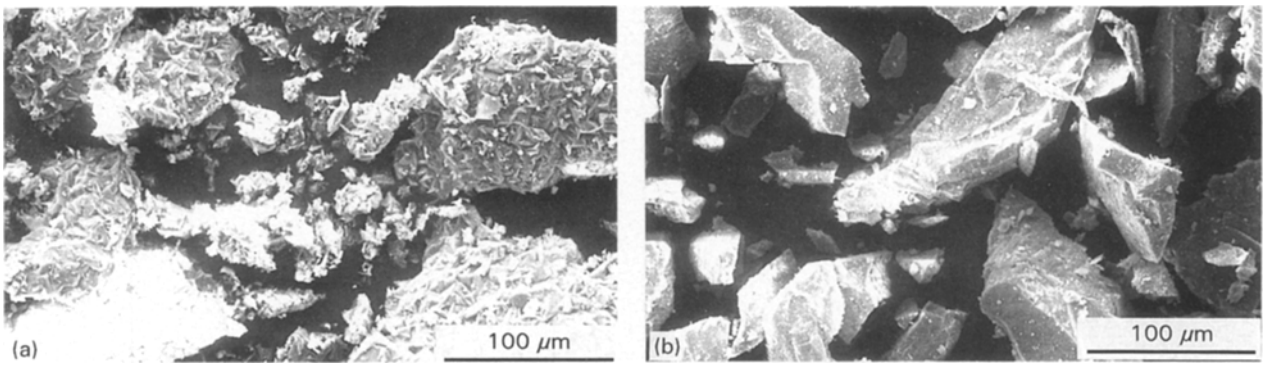

Figure 2 SEM photograph showing the chips of mica glass-ceramic; (a) MACOR sample, cutting rate 4.75 m min^{-1}; (b) Sample 9, cutting rate 3.05 m min^{-1}.

the material removed into smaller particles than the cutting operation. The formation of discontinuous chips during the machining is shown in Fig. 2. The chips are particles with sizes of 1 ~ 500 μm. Thus the machining process for mica glass-ceramics includes both the cutting and the grinding.

For brittle ceramic materials, it is not easy to analyse the effect of each component force on cutting behaviour. It is more convenient to use the total force, F, which can be expressed by the following equation

$$F = (F_P^2 + F_r^2 + F_a^2)^{1/2} \quad (2)$$

The total specific cutting energy, u, is

$$u = Fv/vtb = F/tb \quad (3)$$

where v is linear cutting speed in m min^{-1}, t the depth of cut and b the feed per revolution.

The relationship between u and v is shown in Fig. 3. Linear fittings lead to a simple power-law between u and v such as

$$u = u_1 v^n \quad (4)$$

where u_1 is the cutting energy which can be calculated by extrapolation at $v = 1$ m min^{-1}.

Fig. 4 shows the relationship between the cutting force and the cutting rate of a MACOR® sample and sample 5. Sample 5 (Fig. 4 (b)) shows the decrease in cutting force with an increase in cutting rate up to 40 m min^{-1} and the steep increase at the higher rate. The steep increase in the cutting forces at the high cutting rate resulted from friction between the tool and the workpiece making accurate measurements impossible, and, therefore, the last points were eliminated from the following calculation.

Surface energy can be one main component of cutting energy. Then, the total output specific cutting energy is

$$u = \gamma S + u_s + u_f \quad (5)$$

where γ is the surface energy per unit area, S the surface area per unit volume, u_s the energy of plastic deformation and u_f the energy loss by friction. Mica has a low surface energy along (0 0 1) cleavage plane. The energy required to produce new mica surfaces by cleavage has been found to depend upon the

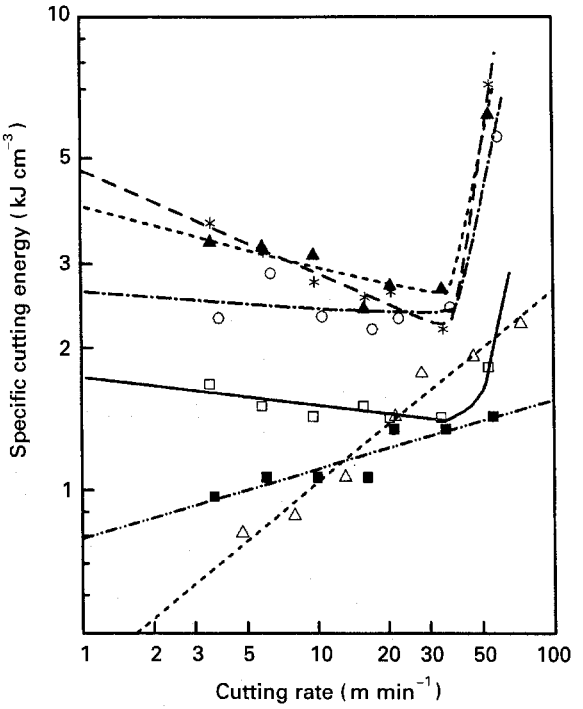

Figure 3 Variation of specific cutting energy with cutting rate for mica glass-ceramics. □, 1; ○, 4; ⁎, 5; ■, 6; ▲, 8; △, 16.

atmosphere. The cleavage energy for muscovite in ultra-high vacuum is 10.2 J m^{-2} while the value measured in air is only 0.3 J m^{-2} [9]. Phlogopite exhibits 2.5 times larger effective surface energy than muscovite, and fluorinated phlogopite has a higher surface energy than OH–phlogopite by about 25% [10, 11]. If we introduce the surface energy of F–phlogopite, then the expected maximum surface energy is about 0.9 J m^{-2}. The fracture surface energies measured by the indentation method are shown in Table I. The energies vary from 9 J m^{-2} to 29 J m^{-2}. The fracture process is more complicated than for single crystals and involves plastic deformation in the zone adjacent to the fracture face, which results in a higher effective surface energy for mica glass-ceramics. The measured specific surface area of MACOR® chips after machining are 2.64 m^2 g^{-1} and 2.45 m^2 g^{-1} at a cutting rate of 4.75 m min^{-1} and 73 m min^{-1}, respectively, which correspond to the surface energy of about 180 J cm^{-3}.

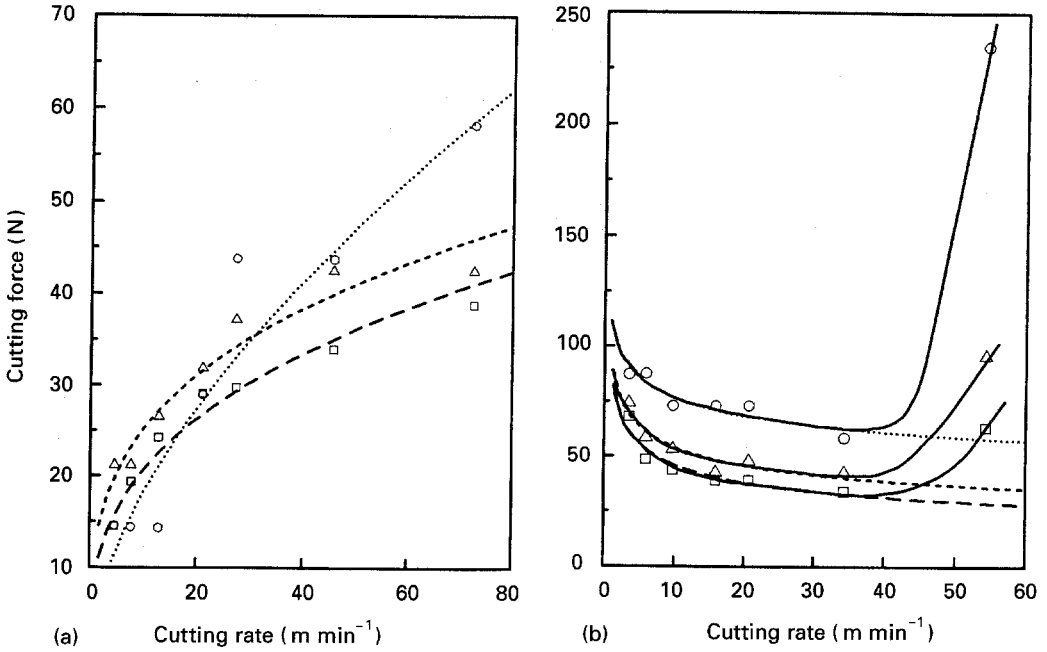

Figure 4 Variation of 3-component cutting forces for mica glass-ceramics (a) with good machinability (MACOR) ○, F_a; △, F_r; □, F_p. and (b) poor machinability; (sample 5). ○, F_r; △, F_a; □, F_p.

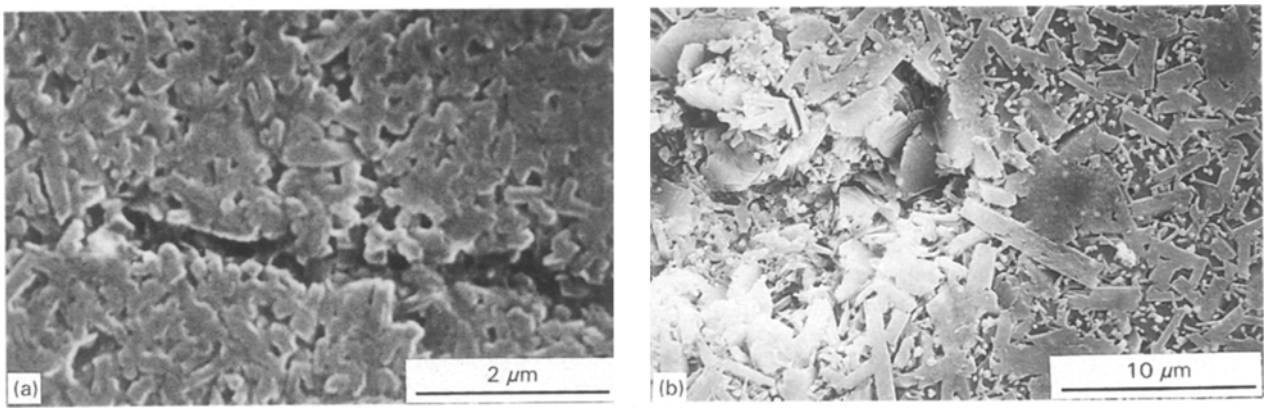

Figure 5 The microstructures of mica glass-ceramics having different machinability; (a) Sample 4, crack path formed by indentation $u_1 = 2587$, $n = -0.03$; (b) Sample 6, disturbed crack propagation by interlocked mica crystals $u_1 = 790$, $n = 0.146$.

There were no differences in the specific surface areas of the chips obtained at different cutting rates. The estimated surface energy is 28% of the total specific cutting energy at a cutting rate of 1 m min^{-1} and 5% at 100 m min^{-1}. One of the main reasons for this difference results from the deflection of the crack path by randomly oriented crystals. Subsidiary cleavages, which can be readily rehealed by cold welding [9], and the deformation and the slip among crystal planes absorb additional energy. In addition, there is a frictional energy which readily changes to heat and sound. Fig. 5 shows the microstructures of glass-ceramics having different machinabilities. For sample 4, a crack propagates between the crystals without severe deflection, while, for sample 6, crack propagation is greatly disturbed by the large mica crystals. For glass-ceramics having disc-shaped particles of high aspect ratio, the fracture surface energy greatly increases due to the crack deflection [12]. The fracture surface energy does not show a direct relationship with the specific cutting energy, but there is a trend of increasing fracture surface energy with increase in machinability.

The specific cutting energy at different cutting rates does not allow accurate comparisons between the materials. A wrong conclusion can be drawn by simply comparing values of the specific cutting energy. Low u value is a necessary condition for good machinability but does not give the information about the quality of machined surface.

From the log–log plot of u and v, it is more convenient to compare slope n among materials to judge the machinability. Fig. 6 shows the relationship between $\log R_{max}$ and n. The measured n values range from -0.2 to 0.5. High n shows the inclination to produce smooth surfaces. A large scattering of the data was originated from the differences in the mechanical strengths and the microstructures. Deryagin and Metsik [10] have observed that the more rapidly the mica specimen is cleaved, the larger is the energy needed to perform the cleavage. They reported that the surface energy reaches a maximum value if the cleaving rate is higher than 3 mm sec^{-1}. Though their

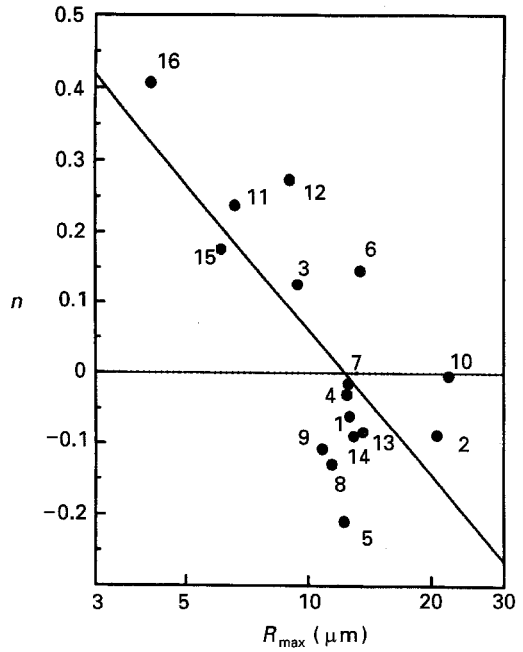

Figure 6 Maximum surface roughness of mica glass-ceramics according to the value of n.

rate is small compared to the cutting rate, we may expect an increase in the cutting force due to this effect. The cutting speed at the tip of the tool is fast but the speeds of cleaving mica crystals can be much smaller according to the direction of crack propagation and the distance from the tip. High speed enlarges the region reached by the cleaving speed having the maximum value of surface energy. This phenomenon can explain the positive exponent n of glass-ceramics with good machinability. Therefore the efficiency for machining depends on the cutting rates and decreases with the increase in cutting rates.

The negative n represents the predominance of the brittle fracture along the glass phase over the continuous delamination through mica crystals. In abrasion data [13], if we consider a specific grinding energy as the sum of kinetic energy of impacting particles on target materials in relation to the volume of target material removed by abrasion, then the specific cutting energy is proportional to $V_p^{-0.4 \sim -1.2}$, where V_p is the impacting velocity of particles, and, therefore, n is $-0.4 \sim -1.2$. Thus the efficiency of grinding increases with the speed. During the cutting operation at high speed, the elastic impact to the workpiece produces sharp fragments, which results in high surface roughness. This effect produces negative n. The material with low crystallinity or poorly interlocked structure due to the spherical shape of mica crystals showed negative values of n.

The specific cutting energy at a low cutting rate of 1 m min^{-1}, the so called "quasi-static condition", is useful to determine the possibility of cutting a workpiece to a thin and feeble section without breaking in the sense of neglecting the elastic impact effect. The materials with a large positive n are machinable with a high precision at $v \to 0$, that is $F \to 0$. On the contrary, the materials with negative n need a large threshold force to start machining, and are not suitable for precise machining. Therefore, it is reasonable to determine the presence of machinability according to the sign of n. For good machinability, the specific cutting energy at low cutting rate (quasi-static condition) should be low, and the exponent n should be positive.

Another criterion for machinability is microhardness, Fig. 7 shows the changes of u_1 and n with the microhardness data. The machinability has a strong dependence on the microhardness. The specific cutting energy can be expressed by the following formula including microhardness H. Similarly to the erosion formula [14], the specific cutting energy is

$$u = AH^m v^n, \tag{6}$$

where A is a constant, and m is an exponent. A well-developed and highly interlocked mica structure has a low microhardness of less than 4 GPa. In this experiment, n depends on the hardness, that is $n = 0.643 - 0.122\,H$. According to this formula if H is lower than 5.2, then n is positive, and the continuous

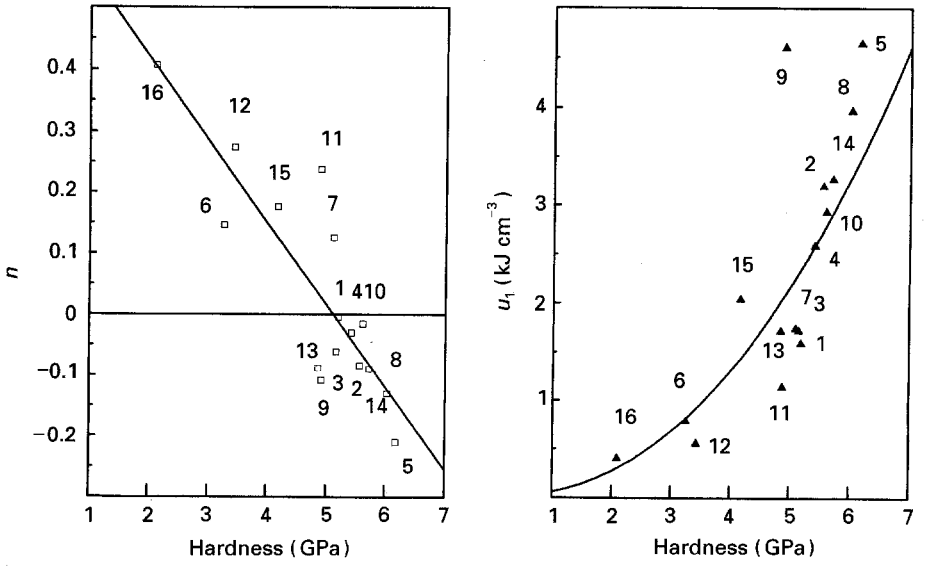

Figure 7 Dependence of parameters n and u_1 on microhardness of mica glass-ceramics.

machining process prevails over the elastic fracture, which can be considered as machinable. Microhardness changes with the volume fraction of mica and the interlocking degree among mica crystals. Thus n is a parameter indicating the tendency of the cutting by the mechanism of cleaving mica. The value m is 2.25 from Fig. 7, which implies a strong dependence on the hardness. In the quasi-static condition $u_1 \propto H^{2.25}$ therefore, the machinability can be predicted by the microhardness data. In addition, the soft characteristic decreases the tool wear and the frictional energy loss. This is essential for the long life of a tool and the wide working range of the cutting rate.

4. Conclusions

Machinability tests on mica glass-ceramics using a tool dynamometer to determine the specific cutting energy draws following conclusions.

1. Specific cutting energy depends on cutting rate and can be expressed by the formula $u = u_1 v^n$.
2. The value u_1 is a reasonable parameter for determination of machinability, because it is the cutting energy at the quasi-static condition, neglecting an elastic impact effect.
3. The exponent n is an indicator related to surface roughness. Positive n indicates the continuous cleavage of mica crystal, which partly originates from the generation of new mica surface.
4. Microhardness is an indirect, but reliable, parameter to compare machinability, which has a relation $u_1 \propto H^{2.25}$. Mica glass-ceramic with a highly interlocked microstructure has a low microhardness and a good machinability.

Acknowledgement

The authors are grateful to the Ministry of Science and Technology of Korea for supporting the present work.

References

1. G. H. BEALL, United States Patent 3 689 293 (1972).
2. D. G. GROSSMAN, United States Patent 3 839 055 (1974).
3. J. F. BEDNARIK and P. W. RICHTER, *Glass Tech.* **27** (1986) 2.
4. M. C. SHAW, "Metal Cutting Principles" (Clarendon Press, Oxford, 1984) p. 137.
5. K. NIHARA, R. MORENA and D. P. H. HASSELMAN, *J. Mater. Sci. Letts.* **1** (1982) 13.
6. R. W. HERTZBERG, "Deformation and Fracture Mechanics of Engineering Materials" (Wiley, New York, 1976) p. 273.
7. L. CERVINKA and J. DUSIL, *J. Non-Crystalline Solids* **21** (1976) 125.
8. S. BRUNAUER, P. EMMETT and E. TELLER, *J. Am. Chem. Soc.* **60** (1938) 309.
9. P. J. BRYANT, in Transactions of the Ninth National Vacuum Symposium. (Pergamon Press, London, 1962) p. 311.
10. B. V. DERYAGIN and M. S. METSIK, *Soviet Phys. Solid State* **1** (1959) 1393.
11. R. F. GIESE, Jr, in "Micas", Reviews in Mineralogy vol. 13, edited by S. W. Bailey (Mineralogical Society of America, 1984) p. 129.
12. K. T. FABER and A. G. EVANS, *Acta Metall.* **31** (1983) 563.
13. S. M. WIEDERHORN and B. J. HOCKEY, *J. Mater. Sci.* **18** (1983) 766.
14. I. J. McCOLM, "Ceramic Hardness" (Plenum Press, New York, 1990) p. 189.

Received 22 October 1993
and accepted 8 September 1994